JOURNAL OF GUIDANCE, CONTROL, AND DYNAMICS
Vol. 20, No. 4, July–August 1997

Numerical Approach to Inverse Flight Dynamics

Marco Borri,* Carlo L. Bottasso,† and Fabio Montelaghi‡
Politecnico di Milano, Milan 20133, Italy

We develop a general numerical approach to inverse problems of vehicle dynamics, suitable for both fixed- and rotating-wing aircrafts. The formulation is based on an energy-preserving finite element in time for rigid body dynamics that ensures unconditional stability according to the energy method. The nonlinear inverse problem of motion is solved by assembling a suitable number of time elements over the time interval of interest and enforcing the appropriate boundary conditions. The capabilities and performance of the proposed procedure are illustrated by means of numerical examples.

Nomenclature

$\mathcal{D}_i$	$= t_i, t_{i+1}$; time element
$\mathrm{d}^\circ(\cdot)/\mathrm{d}t$	= corotational derivative
$\boldsymbol{I}_3, \boldsymbol{I}_6$	= 3×3 and 6×6 identity matrices
$\boldsymbol{J}$	= spatial inertia dyadic
m	= mass
$(O, \boldsymbol{i}_i)$	= fixed frame of origin O, $i = 1, 2, 3$
$(P, \boldsymbol{e}_i)$	= embedded frame of origin P, $i = 1, 2, 3$
$\boldsymbol{p}$	$= \boldsymbol{l}, \boldsymbol{h}$; generalized momentum vector (linear, angular)
$\boldsymbol{R}(\psi)$	= rotation tensor associated with the rotation vector ψ
$\boldsymbol{r}$	$= \boldsymbol{f}, \boldsymbol{m}$; generalized force vector (force, torque)
$\mathcal{T}$	= period of the maneuver
t	= time
$\boldsymbol{w}$	$= \boldsymbol{v}, \boldsymbol{\omega}$; generalized velocity vector (linear, angular)
$\boldsymbol{x}$	$= P - O$; position vector of P in $(O, \boldsymbol{i}_i)$
$\boldsymbol{\alpha}$	= direction cosine matrix
Δt	$= t_{i+1} - t_i$; time step
$\boldsymbol{\delta}$	$= \delta_a, \delta_e, \delta_r, \delta_T$; aileron, elevator, rudder, and thrust controls
$\boldsymbol{\iota}_i, \boldsymbol{\iota}_{i+1}$	= nodal impulses
$(\cdot)_b$	= boundary quantity
$(\cdot)_i$	= quantity pertaining to the ith time node
$(\cdot)^{(j)}$	= quantity pertaining to the jth time element
$\dot{(\cdot)}$	= derivative with respect to time, $\mathrm{d}(\cdot)/\mathrm{d}t$
$\underline{(\cdot)}$	= components in the embedded frame

Introduction

THE general problem of flight simulation includes conventional direct analysis and inverse design of maneuvers. In the case of the direct problem, we are asked to predict the trajectory of the vehicle if the initial conditions and the time history of the controls—for example, three control surfaces and thrust for a conventional airplane—are given. In the case of the inverse problem, we are asked to predict the controls that are compatible with a desired trajectory.

Both topics are of great interest in the context of modern flight mechanics. Typical applications are related to the analysis and design of flight vehicles, for example, the assessment of handling qualities or the design of advanced flight control systems. However, whereas the direct or forward simulation problem can be effectively addressed in a number of ways, the inverse analysis of vehicle motion is a more challenging and computationally intensive task.

Several attempts at solving inverse flight dynamic problems for both fixed-wing aircraft and helicopters are reported in the literature.[1–8] Kato and Sugiura[1] and Thomson and Bradley[2] developed similar inverse techniques based on a differentiation process of the state variables. Although the numerical differentiation approach is prone to numerical instabilities and inaccuracy, these authors successfully applied the methodology to a number of aircraft and helicopter inverse maneuvers. Following a suggestion of Thomson and Bradley,[2] Hess and co-workers[3,6] avoided the numerical difficulties of numerical differentiation by recasting the inverse problem of vehicle motion to one of an integration process, presenting a generalized approach suitable for both fixed- and rotating-wing vehicles. Although more robust than the differentiational gorithm, this methodology occasionally suffers from high-frequency oscillations that have usually been dealt with by means of low-pass digital filtering. More recently, a similar approach was followed by De Matteis et al.[7] that avoided the introduction of filtering through the use of a local optimization procedure.

In this paper, we propose a general numerical approach to inverse flight dynamic problems. Within the framework of finite elements in time, we derive a set of nonlinear discrete equations of motion emanating from a mixed weak principle, which allows the treatment of any well-posed direct and inverse problem.[9] The resulting discrete equations of motion are associated with an energy conservation law that guarantees unconditional stability according to the energy method. Inverse problems are solved by assembling a suitable number of time finite elements over the interval of interest and imposing the appropriate boundary conditions. The resulting discrete equations are nonlinear and are solved by a Newton technique.

In particular, in this work we apply this methodology to the solution of periodic inverse problems. For the purposes of this work, a maneuver is considered periodic when a certain subset of the state of the system (positions, orientations, and velocities) assumes the same values at two distinct time instants. For a rigid vehicle, this class of maneuvers can be used for idealizing a broad range of flight conditions. Clearly, the strict satisfaction of the periodicity condition is seldom encountered in real flight situations. Nevertheless, this model can be a valuable aid in the preliminary design phase and can represent a useful tool in the evaluation of the characteristics and qualities of a vehicle.

We express the problem of vehicle motion in terms of a set of dynamic equations of equilibrium, kinematic relations, and periodicity conditions and a set of other general constraint conditions. The constraint equations can be of different form, depending on the nature of the problem considered. For example, when they specify the time history of the controls and the period of the maneuver, they identify a direct simulation process. When they specify the whole trajectory together with the period of the maneuver, they identify an inverse problem of motion where the number of outputs exceeds the number of inputs. All of the other intermediate cases of interest can be cast in the same general form.

For simplicity, we confine our attention to the "nominal" case, where the number of inputs corresponds to the number of outputs. However, the methodology can be extended to handle the "redundant" case, where the number of outputs is less than the number of

Received June 27, 1996; revision received March 10, 1997; accepted for publication March 17, 1997.

*Professor, Dipartimento di Ingegneria Aerospaziale, Via C. Golgi 40.
†Ricercatore, Dipartimento di Ingegneria Aerospaziale, Via C. Golgi 40.
‡Graduate Student, Dipartimento di Ingegneria Aerospaziale, Via C. Golgi 40; currently Research Engineer, ABB Ricerca S.p.A., Sesto S.G., Milan, Italy.

inputs, adopting a suitable pseudoinversion process as discussed in Ref. 3. This topic will be discussed in a forthcoming paper.

Although in the examples section we restrict our attention to the case of a conventional fixed-wing airplane, we can accommodate within our formulation even helicopters or nonstandard configurations. In fact, the only difference between the two problems is confined to the nonlinear constitutive law that expresses the aerodynamic forces as functions of the system state vector and of the actuators.

We conclude by presenting numerical results obtained with the proposed methodology.

Numerical Analysis of Periodic Problems

We define as "periodic" a maneuver that causes the aircraft to assume the same values of a given subset of its state (position, orientation, and linear and angular velocities) at two distinct time instants. The corresponding time interval $\mathcal{T}$—known or unknown, depending on the problem—is called the period of the maneuver. Letting $(O, \boldsymbol{i}_i)$ $(i = 1, 2, 3)$ be an inertial frame of origin O and $(P, \boldsymbol{e}_i)$ $(i = 1, 2, 3)$ be a frame embedded in the rigid body $\mathcal{B}$, the placement of the body frame is identified at any time $t \in [0, \mathcal{T}]$ by the position vector $\boldsymbol{x}(t) = (P - O)$ of its origin P with respect to the origin O of the inertial frame and by the direction cosine matrix $\boldsymbol{\alpha}(t)$.

An energy-preserving scheme is used for integrating the nonlinear dynamics of a rigid body. Details of the algorithm are given in Ref. 9. Even if energy preservation implies unconditional stability in the nonlinear regime, the method proposed here does not necessarily require the use of this particular time-stepping scheme, and other algorithms might be used, as long as they allow an assembled solution.

For each of the n time elements $\mathcal{D}_i$ in $\mathcal{T}$, the discrete equations of momentum balance referred to the center of mass are

$$\boldsymbol{p}^{(i)} = \boldsymbol{p}_{b_i} + \boldsymbol{\iota}_i \qquad \boldsymbol{p}_{b_{i+1}} = \boldsymbol{p}^{(i)} + \boldsymbol{\iota}_{i+1} \tag{1}$$

$\boldsymbol{p} = (\boldsymbol{l}, \boldsymbol{h})$ being the six-dimensional momentum vector. The symbol $(\cdot)_b$ denotes boundary quantities pertaining to the boundary time instants t_i and t_{i+1}. For a constant interpolation of the generalized force vector $\boldsymbol{r}^{(i)} = (\boldsymbol{f}^{(i)}, \boldsymbol{m}^{(i)})$ within $\mathcal{D}_i$, the force nodal impulses are

$$\boldsymbol{\iota}_i(\boldsymbol{r}) = \boldsymbol{\iota}_{i+i}(\boldsymbol{r}) = \frac{\Delta t^{(i)}}{2}\boldsymbol{r}^{(i)} \tag{2}$$

The constitutive equations that relate velocities and momenta are

$$\begin{aligned} \frac{\boldsymbol{x}_{i+1} - \boldsymbol{x}_i}{\Delta t^{(i)}} &= \frac{\boldsymbol{l}^{(i)}}{m} \\ \boldsymbol{\omega}^{(i)} &= 0.5\boldsymbol{J}_i^{-1}\left[\boldsymbol{R}^T\left(\boldsymbol{\omega}^{(i)}\Delta t^{(i)}\right) + \boldsymbol{I}_3\right]\boldsymbol{h}^{(i)} \end{aligned} \tag{3}$$

The set of equations is completed by the kinematic relations

$$\boldsymbol{\alpha}_{i+1} = \boldsymbol{R}\left(\boldsymbol{\omega}^{(i)}\Delta t^{(i)}\right)\boldsymbol{\alpha}_i \tag{4}$$

Imposing the periodicity conditions

$$\boldsymbol{p}_{b_1} = \boldsymbol{p}_{b_{n+1}} \qquad \boldsymbol{\alpha}_1 = \boldsymbol{\alpha}_{n+1} \tag{5}$$

and assembling over the period, the discrete equations of motion (1) and (4) can be rewritten as

$$\begin{aligned} \boldsymbol{p}^{(1)} - \boldsymbol{p}^{(n)} &= 0.5\left(\Delta t^{(n)}\boldsymbol{r}^{(n)} + \Delta t^{(1)}\boldsymbol{r}^{(1)}\right) \\ \boldsymbol{p}^{(2)} - \boldsymbol{p}^{(1)} &= 0.5\left(\Delta t^{(1)}\boldsymbol{r}^{(1)} + \Delta t^{(2)}\boldsymbol{r}^{(2)}\right) \\ &\vdots \\ \boldsymbol{p}^{(n)} - \boldsymbol{p}^{(n-1)} &= 0.5\left(\Delta t^{(n-1)}\boldsymbol{r}^{(n-1)} + \Delta t^{(n)}\boldsymbol{r}^{(n)}\right) \end{aligned} \tag{6}$$

and

$$\begin{aligned} \boldsymbol{\alpha}_2 &= \boldsymbol{R}\left(\boldsymbol{\omega}^{(1)}\Delta t^{(1)}\right)\boldsymbol{\alpha}_1 \\ \boldsymbol{\alpha}_3 &= \boldsymbol{R}\left(\boldsymbol{\omega}^{(2)}\Delta t^{(2)}\right)\boldsymbol{\alpha}_2 \\ &\vdots \\ \boldsymbol{\alpha}_1 &= \boldsymbol{R}\left(\boldsymbol{\omega}^{(n)}\Delta t^{(n)}\right)\boldsymbol{\alpha}_n \end{aligned} \tag{7}$$

Equations (6) can be written in compact form as

$$\mathcal{P}\boldsymbol{p}_g = \mathcal{R}\boldsymbol{r}_g \tag{8}$$

where $\boldsymbol{p}_g$ and $\boldsymbol{r}_g$ denote the vectors built, arranging sequentially from the first time element to the last one the generalized momenta and the generalized external forces. $\mathcal{P}$ and $\mathcal{R}$ are square matrices of order $6 \times n$. $\mathcal{P}$ is obtained by placing n identity matrices $\boldsymbol{I}_6$ of size 6×6 on the principal diagonal and $n - 1$ matrices $-\boldsymbol{I}_6$ on the lower diagonal. The imposition of the periodicity condition places an additional $-\boldsymbol{I}_6$ matrix in the upper-right-hand corner of $\mathcal{P}$. $\mathcal{R}$ presents a similar structure. Considering, for example, $n = 4$, $\mathcal{P}$ is

$$\mathcal{P} = \begin{bmatrix} \boldsymbol{I}_6 & 0 & 0 & -\boldsymbol{I}_6 \\ -\boldsymbol{I}_6 & \boldsymbol{I}_6 & 0 & 0 \\ 0 & -\boldsymbol{I}_6 & \boldsymbol{I}_6 & 0 \\ 0 & 0 & -\boldsymbol{I}_6 & \boldsymbol{I}_6 \end{bmatrix} \tag{9}$$

whereas $\mathcal{R}$ is

$$\mathcal{R} = 0.5\begin{bmatrix} \Delta t^{(1)}\boldsymbol{I}_6 & 0 & 0 & \Delta t^{(4)}\boldsymbol{I}_6 \\ \Delta t^{(1)}\boldsymbol{I}_6 & \Delta t^{(2)}\boldsymbol{I}_6 & 0 & 0 \\ 0 & \Delta t^{(2)}\boldsymbol{I}_6 & \Delta t^{(3)}\boldsymbol{I}_6 & 0 \\ 0 & 0 & \Delta t^{(3)}\boldsymbol{I}_6 & \Delta t^{(4)}\boldsymbol{I}_6 \end{bmatrix} \tag{10}$$

When using a constant interpolation of the external generalized forces, the number of assembled time elements in $\mathcal{T}$ must be odd. In fact, the use of an even number of elements causes the appearance of spurious modes in the solution, causing $\mathcal{R}$ to be singular. This is a known phenomenon of discretization.[10]

Periodic Inverse Flight Dynamics

Constraint Conditions

The set of discrete equations for the periodic inverse problem of vehicle motion was derived in the preceding section and includes for each time element the equations of dynamic equilibrium (1) and the constitutive equations (3) and for each time node the kinematic relations (4). These equations can be augmented by a set of constraint conditions

$$\mathcal{C}(\boldsymbol{\alpha}, \boldsymbol{w}, \boldsymbol{\delta}, \mathcal{T}) = 0 \tag{11}$$

In general, these equations can be regarded as functions of the orientation $\boldsymbol{\alpha}$, the generalized velocity $\boldsymbol{w}$, the controls $\boldsymbol{\delta}$, and the maneuver period $\mathcal{T}$. In the nominal case, there are n such equations, where n is the number of time finite elements assembled in $\mathcal{T}$. These equations can assume different forms in correspondence to different problems of inverse motion. For example, they might specify the time history of a rotation vector component in the case of a roll maneuver, or they might specify a known value of the period or a known time history of some of the controls, e.g., a constant value of the throttle. In the numerical example section, we present a few different forms for Eq. (11). Clearly, even the forward simulation problem can be modeled by the same set of relations, when Eq. (11) specifies the time history of all of the controls. In practice, the constraint conditions play the role of defining the nature of the problem considered.

Force Constitutive Models

The problem definition is completed by the introduction of a suitable constitutive model that relates the external generalized forces to the controls and the system state vector. The external forces $\boldsymbol{f}$ acting on a flying vehicle and referred to the center of mass can be regarded as composed of two parts, namely the weight $m\boldsymbol{g}$ and the aerodynamic forces $\boldsymbol{A}$ including the forces of propulsive origin, i.e.,

$$\boldsymbol{f} = m\boldsymbol{g} + \boldsymbol{A} \tag{12}$$

The external torques $\boldsymbol{G}$ are of a purely aerodynamic-propulsive nature. The aerodynamic forces $\boldsymbol{A}$ and torques $\boldsymbol{G}$ normally depend on the local ambient density, the present and past motion of the vehicle relative to the atmosphere, and the actuation of the controls. For simplicity, we restrict our attention to the steady model. In this case,

the constitutive equations of the aerodynamic generalized forces referred to a fixed frame can be expressed as

$$\boldsymbol{A} = \alpha\bar{\boldsymbol{A}}(\bar{\boldsymbol{v}}, \dot{\bar{\boldsymbol{v}}}, \bar{\boldsymbol{\omega}}, \boldsymbol{\delta}, \boldsymbol{\sigma}) \qquad \boldsymbol{G} = \alpha\bar{\boldsymbol{G}}(\bar{\boldsymbol{v}}, \dot{\bar{\boldsymbol{v}}}, \bar{\boldsymbol{\omega}}, \boldsymbol{\delta}, \boldsymbol{\sigma}) \tag{13}$$

where the bar over the symbols indicates quantities in body frame and $\bar{\boldsymbol{v}} = (u, v, w)$, $\bar{\boldsymbol{\omega}} = (p, q, r)$, $\bar{\boldsymbol{A}} = (X, Y, Z)$, and $\bar{\boldsymbol{G}} = (L, M, N)$; $\boldsymbol{\sigma}$ is a set of parameters that influence the aerodynamic reactions, for example, the air density and gust factors.

The problem is nonlinear because of the constitutive equation for the angular momenta $\boldsymbol{h}$, because of the generalized aerodynamic forces, and, in general, because of the constraint conditions [Eq. (11)]. Consistent linearization with respect to the unknown parameters allows us to adopt an iterative Newton-like procedure. The resulting linearized system of equations is written in terms of increments of displacements, rotation, linear and angular velocities for each time node, and increments of controls and time step sizes for each time element.

Computation of the Tentative Solution

The Newton solution process is initiated by specifying a first tentative solution. The choice of a tentative solution that represents a good approximation of the final one will allow convergence in fewer iterations. However, as long as the initial guess is within the basin of attraction of the nonlinear solution process, the final solution will not depend on the tentative one.

In this work, we propose to compute the first tentative solution by trimming the aircraft at every time node. The trimmed condition is identified in correspondence to the steady maneuver that provides a suitable approximation to the problem considered. We define as steady a maneuver such that

$$\frac{\mathrm{d}^{\circ}\boldsymbol{w}}{\mathrm{d}t} = 0 \tag{14}$$

Equation (14) implies

$$\boldsymbol{T}_0(\boldsymbol{p})\boldsymbol{w} = \boldsymbol{r} \tag{15}$$

where the operator $\boldsymbol{T}_0(\cdot)$ applied to $\boldsymbol{p}$ is

$$\boldsymbol{T}_0(\boldsymbol{p}) = \begin{bmatrix} 0 & \boldsymbol{l} \times \boldsymbol{I}_3 \\ \boldsymbol{l} \times \boldsymbol{I}_3 & \boldsymbol{h} \times \boldsymbol{I}_3 \end{bmatrix} \tag{16}$$

Equation (15) states that a general steady maneuver is one for which the gyroscopic forces $\boldsymbol{T}_0(\boldsymbol{p})\boldsymbol{w}$ are in equilibrium with the external forces $\boldsymbol{r}$. Consequently, it follows that the most general steady maneuver is characterized by a helicoidal trajectory with axis parallel to the angular velocity vector $\boldsymbol{\omega}$.

Equation (15) is augmented with the additional piloting condition that can be formally expressed as

$$\mathcal{C}(\boldsymbol{\alpha}, \boldsymbol{w}, \boldsymbol{\delta}) = 0 \tag{17}$$

A typical example of the form assumed by Eq. (17) is given by the symmetric flight condition, where the linear velocity vector lies in the plane of symmetry of the vehicle. Indicating with $\boldsymbol{e}_2$ the unitary vector perpendicular to the plane of symmetry, Eq. (17) in this case is

$$\boldsymbol{v} \cdot \boldsymbol{e}_2 = 0$$

Equations (15) and (17) are nonlinear and are solved with a Newton procedure.

Once the trimmed condition has been obtained, the assembled inverse procedure is initiated. At each iteration, the system unknowns are updated in terms of the computed increments. The iterative procedure is continued until convergence to the prescribed level of accuracy.

Numerical Results

In this section, we apply the developed procedures to a number of inverse problems of aircraft motion, and we assess their performance characteristics. We consider an A4D aircraft characterized by the aerodynamic data published in Ref. 11 for the flight condition relative to 15,000 ft and 634 ft/s. The emphasis of the exercises is on showing the ability of the procedure in dealing with complex nonlinear inverse problems rather than on the issue of modeling real flight maneuvers. This justifies the choice of a simple aerodynamic model. Clearly, more complicated models could be used without altering the algorithmic approach.

All of the results have been validated by using the computed controls for performing a direct simulation and comparing the resulting trajectory with the nominal one. Excellent agreement between the real and computed trajectories has been observed in all of the test cases analyzed.

For simplicity, we consider discretizations denoted by a constant value of the time step size. However, it is clear that the use of an adaptive time-stepping process could greatly enhance the performance of the method in some cases.

Straight Roll of 360 deg

This example was first presented by Kato and Sugiura.[1] Here, the goal of the exercise is to validate the procedures by comparing the results with those of other known approaches. Although the maneuver is of little interest from the point of view of flight mechanics, it represents a valid test case for a numerical approach because it is characterized by large-amplitude variations of all of the controls.

The problem deals with a maneuver in which the airplane describes a straight trajectory while performing a 360-deg continuous roll. The roll angle as a function of time is given by

$$\varphi(t) = (2\pi/16)\{\cos(3\pi t/T) - 9\cos(\pi t/T) + 8\} \tag{18}$$

The period to complete a 360-deg roll is $\mathcal{T} = 6$ s.

The temporal discretization makes use of 61 time elements. A first tentative solution was computed by trimming the aircraft at each time node with the constant linear velocity and the angular velocity corresponding to Eq. (18). Convergence to the trimmed solution was obtained in four Newton iterations on average, having set a tolerance of 10^{-10} on the energy norm of the residual. The periodic solution was then computed with the technique described in the preceding sections, using the tentative solution as an initial guess. The tolerance was set equal to the one used for the trimmed solution. Convergence was achieved in four Newton iterations.

Figures 1–6 report the amplitudes of the angles of attack and sideslip and of the aileron, elevator, rudder, and thrust deflections. All of the plots show the dynamic solution (thick lines) and the initial tentative solution corresponding to the trimmed condition (thin lines). The magnitude of the deflections is certainly too large for the simple linear aerodynamic model adopted. However, the

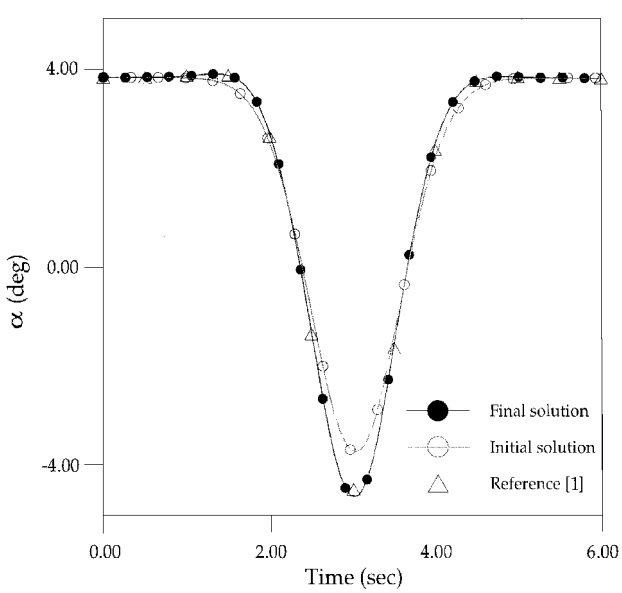

Fig. 1 Straight-roll (360 deg) maneuver: angle of attack.

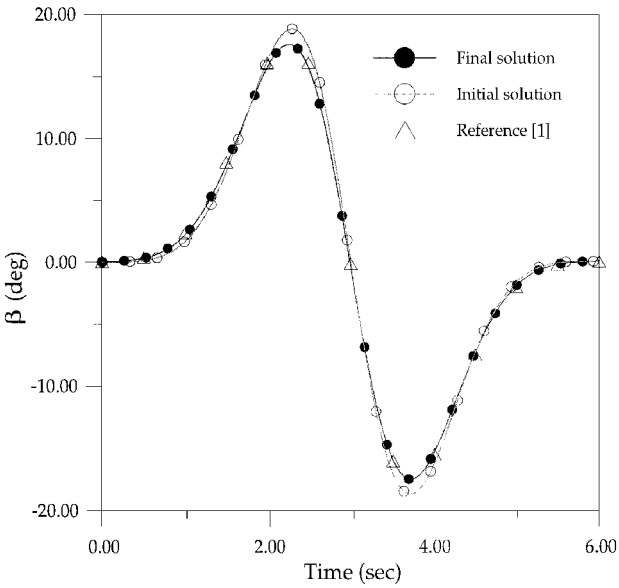

Fig. 2 Straight-roll (360 deg) maneuver: sideslip angle.

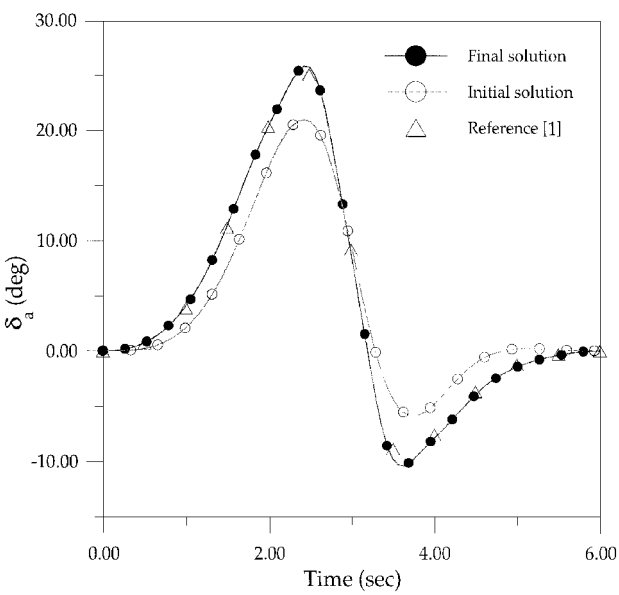

Fig. 3 Straight-roll (360 deg) maneuver: aileron deflection.

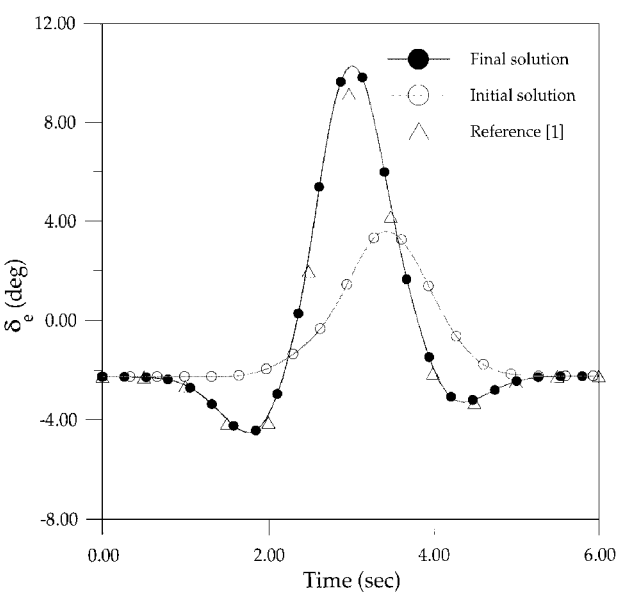

Fig. 4 Straight-roll (360 deg) maneuver: elevator deflection.

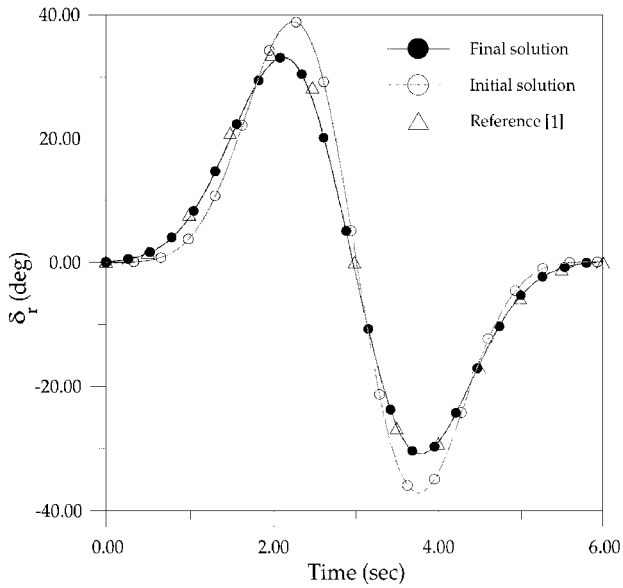

Fig. 5 Straight-roll (360 deg) maneuver: rudder deflection.

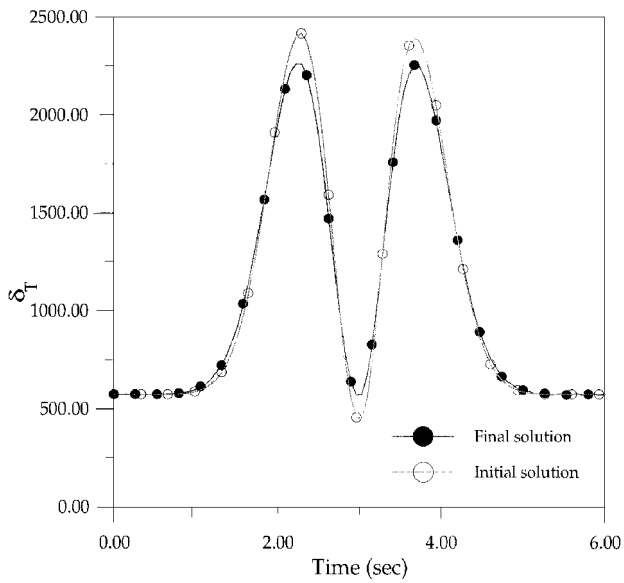

Fig. 6 Straight-roll (360 deg) maneuver: thrust level.

aspect of identifying a suitable model for dealing with this class of maneuvers is outside the scope of the present work.

To validate the results against a known procedure, we have implemented the approach developed in Ref. 1. The results obtained are presented together with our solution in Figs. 3–5. For the present model problem, a good agreement between the two approaches can be appreciated. However, we note that there is a significant difference between the two methods with respect to this example. In fact, our algorithm is based on a standard finite element discretization process, and therefore it is convergent, in the sense that a finer temporal discretization yields more accurate results. On the contrary, when we tried to reduce the time step size for the algorithm of Ref. 1, we observed an unstable behavior that prevented us from obtaining a solution.

Helicoidal Roll of 360 deg

In this roll maneuver, the trajectory is a helix of radius $R = 50$ ft, pitch $p = 7608$ ft, and period $\mathcal{T} = 12$ s. The position vector $\boldsymbol{x}(t)$ is given by

$$\boldsymbol{x} = \{(p/\mathcal{T})t,\ R\cos[\chi(t)],\ R\sin[\chi(t)]\} \tag{19}$$

The angle χ varies linearly with time, as given by

$$\chi(t) = (2\pi/\mathcal{T})t \tag{20}$$

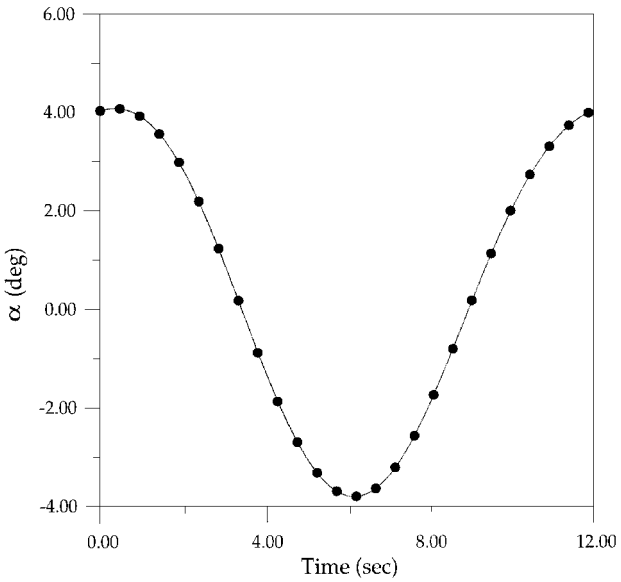

Fig. 7 Helicoidal-roll (360 deg) maneuver: angle of attack.

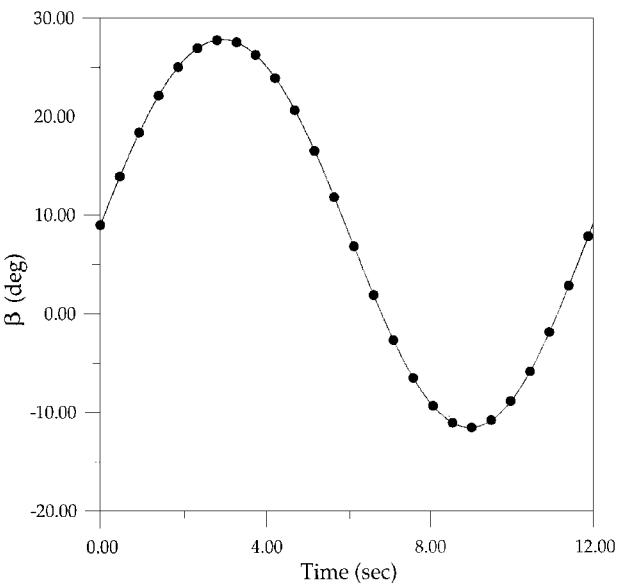

Fig. 8 Helicoidal-roll (360 deg) maneuver: sideslip angle.

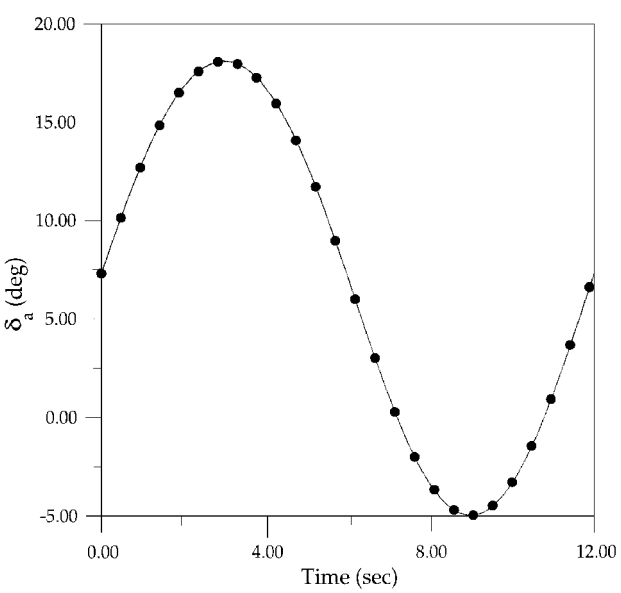

Fig. 9 Helicoidal-roll (360 deg) maneuver: aileron deflection.

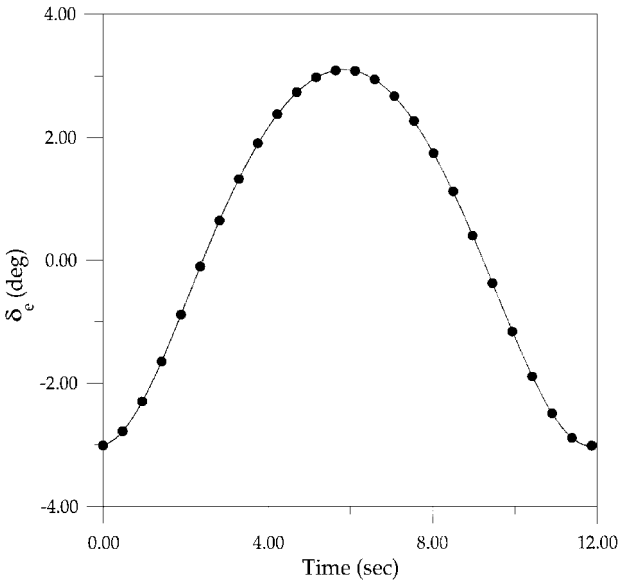

Fig. 10 Helicoidal-roll (360 deg) maneuver: elevator deflection.

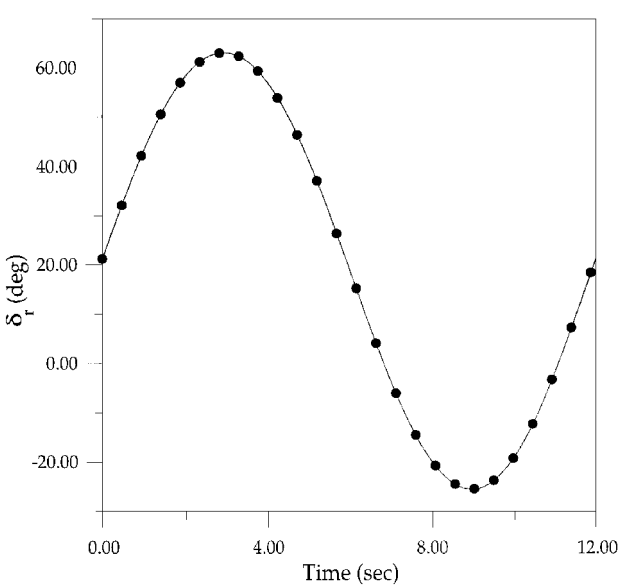

Fig. 11 Helicoidal-roll (360 deg) maneuver: rudder deflection.

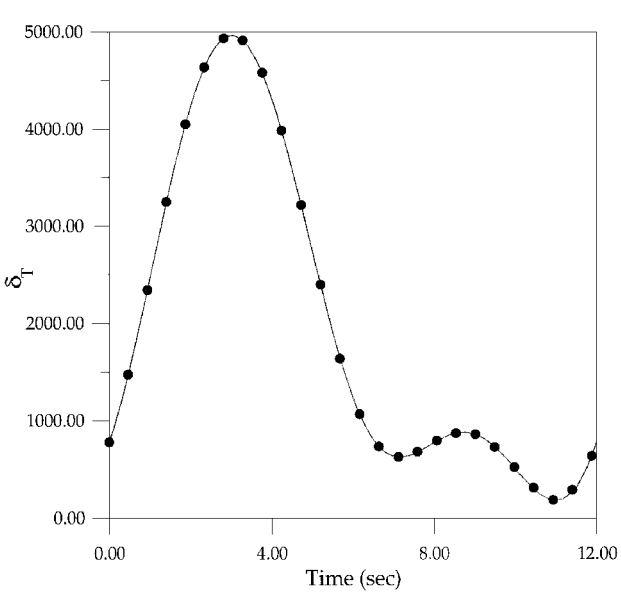

Fig. 12 Helicoidal-roll (360 deg) maneuver: thrust level.

A different form of the constraint condition is used in this case. Instead of setting the roll angle as in the preceding exercise, we impose that the unit vector $\boldsymbol{e}_2$ always remains perpendicular to the unit vector $\boldsymbol{e}_0$, where

$$\boldsymbol{e}_0 = \boldsymbol{R}[\chi(t)\boldsymbol{i}_1]\boldsymbol{i}_3 \tag{21}$$

Therefore, the unit vector $\boldsymbol{e}_0$ is constrained to lie in the symmetry plane of the aircraft.

The temporal discretization makes use of 101 time finite elements. The solution procedure is analogous to the one adopted in the preceding example, and the convergence tolerance on the energy norm of the residual was set to 10^{-10}.

Figures 7–12 report the amplitudes of the angles of attack and sideslip and of the aileron, elevator, rudder, and thrust deflections. Even in this case, the system response is characterized by large variations of all of the quantities.

Conclusions

We have presented a formulation for analyzing inverse problems of rigid vehicle motion. The algorithm is general because no assumption on the vehicle characteristics and configuration is implied in the formulation. Therefore, it is suitable for both fixed- and rotating-wing aircrafts. The new methodology has been applied to the study of periodic maneuvers. The introduction of aerodynamic models more sophisticated than the one considered here is possible, and it would require only a different definition of the constitutive model that relates the external forces to the system-state vector and controls.

The approach is based on the use of an energy-preserving algorithm for nonlinear rigid body dynamics. A suitable number of time finite elements is assembled over the period of interest—period of known or unknown length, depending on the problem considered—and the periodicity conditions are imposed in the usual fashion by folding the corresponding rows and columns of the assembled system matrices. The solution is obtained by using a Newton iterative procedure with consistent linearization of the discrete equations.

The procedures have been illustrated on some nominal fixed-wing aircraft inverse problems, and the main features of the proposed approach have been verified.

References

[1] Kato, O., and Sugiura, I., "An Interpretation of Airplane General Motion and Control as Inverse Problem," *Journal of Guidance, Control, and Dynamics,* Vol. 9, No. 2, 1986, pp. 198–204.

[2] Thomson, D. G., and Bradley, R., "Development and Verification of an Algorithm for Helicopter Inverse Simulations," *Vertica*, Vol. 14, No. 2, 1990, pp. 185–200.

[3] Hess, R. A., Gao, C., and Wang, S. H., "Generalized Technique for Inverse Simulation Applied to Aircraft Maneuvers," *Journal of Guidance, Control, and Dynamics*, Vol. 14, No. 5, 1991, pp. 920–926.

[4] Sentoh, E., and Bryson, A., "Inverse and Optimal Control for Desired Output," *Journal of Guidance, Control, and Dynamics*, Vol. 15, No. 3, 1992, pp. 687–691.

[5] Snell, S. A., Enns, D. F., and Garrard, W. L., "Non-Linear Inversion Flight Control for a Supermaneuverable Aircraft," *Journal of Guidance, Control, and Dynamics*, Vol. 15, No. 4, 1992, pp. 976–984.

[6] Hess, R. A., and Gao, C., "A Generalized Algorithm for Inverse Simulation Applied to Helicopter Maneuvering Flight," *Journal of the American Helicopter Society*, Vol. 38, No. 4, 1993, pp. 3–15.

[7] De Matteis, G., De Socio, L. M., and Leonessa, A., "Solution of Aircraft Inverse Problems by Local Optimization," *Journal of Guidance, Control, and Dynamics*, Vol. 18, No. 3, 1995, pp. 567–571.

[8] Rutherford, S., and Thomson, D. G., "Improved Methodology for Inverse Simulation," *Aeronautical Journal*, Vol. 100, No. 993, 1996, pp. 79–86.

[9] Borri, M., and Bottasso, C. L., "Petrov–Galerkin Finite Elements in Time for Rigid Body Dynamics," *Journal of Guidance, Control, and Dynamics*, Vol. 17, No. 5, 1994, pp. 1061–1067.

[10] Bottasso, C. L., "A Non-Linear Beam Space-Time Formulation Using Quaternion Algebra: Interpolation of the Lagrange Multipliers and the Appearance of Spurious Modes," *Computational Mechanics*, Vol. 10, No. 5, 1992, pp. 359–368.

[11] McRuer, D., Ashikenas, I., and Graham, D., *Aircraft Dynamics and Automatic Control*, Princeton Univ. Press, Princeton, NJ, 1973, pp. 701–704.